36

The Simulation of Liquid Helium.

D. M. CEPERLEY

Lawrence Livermore National Laboratory - Livermore, CA 94550

1. – Introduction.

I am going to discuss a somewhat different topic than the main focus of this school, namely simulation methods for quantum-mechanical systems at finite temperatures. Recently it has been shown that static properties of some quantum systems can be obtained by simulation in a straightforward manner using path integrals, albeit with an order of magnitude more computing effort needed than for the corresponding classical systems. Some dynamical information can be gleaned from these simulations as will be discussed below. But this is very limited—there is no quantum version of the molecular-dynamics method.

The path integral method will be illustrated by discussing the application to liquid helium. This system was chosen because, firstly, the interaction potential between helium atoms is well understood, at least for temperatures of less than 10^4 K and pressures of less than 1 Mbar. Thus one can make an unambiguous comparison with the wealth of thermodynamic and scattering properties which have been measured. The Aziz [1] potential (HFDHE2) between all pairs of helium atoms was assumed. This is a short-ranged interaction and so only a minimum number of atoms are needed in the simulation to calculate most of the properties of bulk helium. Secondly, there has been a great deal of theoretical work on liquid helium. The picture directly related to the simulation method is that of Feynman [2]. Also there are simulation results at zero temperature [3] with which to compare. Finally there are still many interesting unresolved questions: the detailed form of the momentum distribution, the details of exchange in crystal helium 3, the form of the interface between liquid and solid helium. However, the simulations of liquid helium were primarily undertaken to establish confidence in the path integral method, to show that one can indeed obtain exact results at finite temperature for a strongly interacting quantum many-body system. Then one can proceed on to more complex and less understood systems.

2. – The density matrix.

Let us first review some of the basic properties of the density matrix, that operator which is needed to calculate any property of a quantum system at finite temperature. In operator notation the density matrix is $\exp[-\beta H]$, where $\beta = 1/kT$, T is the temperature and H is the Hamiltonian. Any observable O is obtained as

$$\langle O \rangle = \mathrm{tr}\,[O \exp[-\beta H]]/\mathrm{tr}\,[\exp[-\beta H]]\,. \tag{2.1}$$

If one can simulate the density matrix, that is sample co-ordinates R and R' (R refers to a point in the $3N$-dimensional co-ordinate space) for the density $\langle R \exp[-\beta H] R' \rangle$, then one can calculate any static property just as with classical systems. The brackets mean just to evaluate the density matrix between those points. The full density matrix in co-ordinate space is a function of $6N$ variables. The diagonal part of the density matrix is obtained when $R = R'$. Scalar properties such as the radial distribution function and the potential energy are determined only by the diagonal elements of the density matrix. Simulations off the diagonal are necessary to determine the momentum distribution.

One can obtain the density matrix at low temperatures by inserting a complete set of eigenstates $\varphi_n(R)$ with eigenvalues E_n:

$$\langle R \exp[-\beta H] R' \rangle = \sum_{n=1}^{\infty} \varphi_n^*(R) \exp[-\beta E_n] \varphi_n(R')\,. \tag{2.2}$$

Thus on the diagonal at low temperatures the density matrix goes to the square of the ground-state wave function.

On the other hand, at a sufficiently high temperature, the kinetic- and potential-energy operators can be allowed to commute and the density matrix can be evaluated as

$$\langle R \exp[-\beta H] R' \rangle = \langle R \exp[-\beta T] R' \rangle \exp\left[-\beta/2\{V(R) + V(R')\}\right]. \tag{2.3}$$

The first factor on the right-hand side is the density matrix for an ideal gas and has the explicit form of a Gaussian in $R - R'$:

$$\langle R \exp[-\beta T] R' \rangle = (4\pi D\beta)^{-3N/2} \exp[-(R - R')^2/4D\beta]\,, \tag{2.4}$$

where $D = \hbar^2/2m$. At high temperature the density matrix goes to the classical Boltzmann distribution, times a factor which keeps R and R' close and has the form of a harmonic spring potential. The spring constant gets tighter

and tighter as the temperature is increased. The thermal wavelength, equal to $(2D\beta)^{\frac{1}{2}}$, gives the spatial extent of quantum effects.

In order to simulate helium at low temperatures one uses the simple properties of an exponential operator:

$$\langle R_0 \exp[-\beta H] R_M\rangle = \langle R_0 \exp[-\tau H] R_1\rangle \langle \ldots\rangle \langle R_{M-1} \exp[-\tau H] R_M\rangle , \tag{2.5}$$

where the intermediate co-ordinates $R_1, \ldots, R_{M-1}$ are to be integrated over and $\tau = \beta/M$. Then, if M is large enough, one can use eq. (2.3) for the density matrix although in practice it is necessary to improve that approximation as will be discussed shortly. Equation (2.5) is the basis of the path integral method. One simply considers the expression on the right-hand side as a « classical » distribution to be sampled and $R_1, \ldots, R_{M-1}$ have an equal footing with R_0 and R_M. For the calculation of scalar observables, such as the potential energy, the diagonal part of the density matrix is needed and thus $R_0 = R_M$. Thus there are $3N \times M$ co-ordinates to sample instead of just $3N$ for a classical Monte Carlo simulation.

Such a « classical » distribution is very much like a system of N ring polymers at a temperature $T \times M$, made up from M « monomers ». The subscripts identify the monomer, they are also referred to as time slices (really imaginary time). Only monomers at the same time interact with each other with the potential $\tau V(r_{ij})$.

The other picture, due to FEYNMAN [1] and KAC [4], is of a random walk or path integral. If we take the limit as $M \to \infty$ of eq. (2.5), then the kinetic-energy operators describe a random walk starting at R_0, and ending at R_M and lasting a time β. The density matrix is equal to the average over all such walks of the free-particle density matrix times the exponential of the integrated potential along that walk:

$$\langle R_0 \exp[-\beta H] R_M\rangle = \langle R_0 \exp[-\beta T] R_M\rangle \overline{\left\langle \exp\left[-\int_0^\infty \mathrm{d}t \sum_{i<j} V(r_{ij}(t))\right]\right\rangle} . \tag{2.6}$$

The efficiency of the simulation will depend on the value of τ for which one can write down a good form for the density matrix. It turns out for helium the simple classical form of eq. (2.3) will be accurate enough only if $\tau < 0.001/\mathrm{K}$. This means for simulations in superfluid helium at 2 K that each polymer will have 500 monomers, which is very inefficient. One can do much better by solving the two-atom problem exactly and obtaining a pair product form [5] for the density matrix by assuming the average of the products in eq. (2.6) is equal to the product of the averages:

$$\langle R_0 \exp[-\beta H] R_M\rangle = \langle R_0 \exp[-\beta T] R_M\rangle \prod_{i<j} \overline{\left\langle \exp\left[-\int_0^\infty \mathrm{d}t V(r_{ij}(t))\right]\right\rangle} . \tag{2.7}$$

The error in this density matrix comes only from three- and higher-body scattering. It has been found that this pair product density matrix is sufficiently accurate for $\tau < 0.025/\mathrm{K}$ which leads to a substantially more efficient algorithm than one based on the semi-classical density matrix. The tabulation of the pair density matrices at a variety of temperatures is carried out by specialized numerical techniques [5].

The boson density matrix is defined by restricting the sum in eq. (2.2) to be only over fully symmetric states and can be obtained from the density matrix for distinguishable particles by symmetrizing with respect to particle co-ordinates

$$\langle R \exp[-\beta H] R' \rangle_{\text{boson}} = \sum_P \langle PR \exp[-\beta H] R' \rangle / N! \tag{2.8}$$

since all eigenfunctions which are not fully symmetric will disappear. In our classical analogy, the polymers can become cross-linked. To calculate properties on the diagonal, the random walks no longer must return to their starting places but to any other walk's starting place. It is like the game of musical chairs. The superfluid transition is driven by this indistinguishability which serves to connect superfluid helium macroscopically just as jello changes phase when it cools and its molecules cross-link. The transition happens when the thermal wavelength becomes approximately equal to the interparticle spacing. The task of the Monte Carlo algorithm is then plain, it is to effectively sample this combined space $\{R^{3NM} P_N\}$, where P_N is the permutation group. That is to sample all energetically favorable polymers and all the cross-linked possibilities.

3. – The Monte Carlo method.

The Metropolis algorithm [6] is almost universally used to evaluate ratios of integrals as in eq. (2.1). Let $\Pi(s)$ be the normalized distribution in eqs. (2.5)-(2.8), where s refers to all of the $3N \times M \times P$ co-ordinates. The Metropolis algorithm samples by setting up a Markov chain with the detailed-balance property

$$\Pi(s) P(s \to s') = \Pi(s') P(s' \to s) , \tag{3.1}$$

where P is the probability of making a transition from one state to another. A trial move to a nearby point s' is made based on some assumed probability function $\hat{P}(s')$. Then the trial move is accepted with probability equal to

$$a = \min\{1, \Pi(s') \hat{P}(s) / \Pi(s) \hat{P}(s')\} \tag{3.2}$$

which will guarantee that eq. (3.1) is obeyed for $P = a\hat{P}$. The algorithm is guaranteed **to converge to Π, but the convergence time is governed by the**

transition probabilities and it can be very slow, particularly for this type of distribution. After all, relaxation times for real polymers can be seconds, or days.

Now a naive scheme, taken over directly from the simulation of classical liquids, would be simply to take $\hat{P}$ uniform about s within a cube for only one monomer. While that would be effective for nearly classical systems, it would be excruciatingly slow at low temperatures, assuming M is large. The reason is that the springs from the nearby links of the polymer constrain any one link, so that motion of the ring as a whole would be very slow. For bosons one must make permutation moves as well as spatial moves, and those necessarily involve moving many links of at least 2 atoms together with the permutation move. In other words, an efficient algorithm for quantum systems at low temperatures must involve moving simultaneously many monomers.

The results to be discussed here were obtained by moving the co-ordinates of from 1 to 4 atoms in 4 to 8 time slices together with a permutation move to be discussed next. Now the conditional probability distribution of a point R, at time t, part way through a random walk of length t, which begins at R_1 and ends at R_2, is given by the conditional distribution

$$f(R) = \langle R_1 \exp[-tH]R\rangle \langle R \exp[-(\beta - t)H]R_2\rangle / \langle R_1 \exp[-\beta H]R_2\rangle \,. \tag{3.3}$$

Note that the integral over R of f is unity, so it is a probability distribution from which points R can be sampled. One can approximate f sufficiently accurately so that many co-ordinates may be sampled together with a high acceptance probability. But this means that an expression is needed for the density matrix, not just at the high temperature τ, but all the way down to the temperature appropriate to the size of moves to be made, which will equal something like twice the lambda temperature or 4 K, if permutation moves are to be accepted. However, only the density matrix at time τ will affect the converged results, the lower-temperature density matrices will affect only the rate of convergence of the random walk and hence the error bars. For the ideal gas, $f(R)$ is a Gaussian, one whose center moves in a straight line from R_1 to R_2, and whose width slowly spreads at the beginning of the walk and then contracts. Turning on the interaction in addition makes the regions where two monomers overlap forbidden. It is convenient to approximate f by a multivariate Gaussian (one with cross-correlations) since a Gaussian can be rapidly sampled. Again such an approximation only affects the error bars on the final answers, not the limiting results.

The basic principles of sampling permutations are the same as those for sampling spatial moves except permutations are in discrete space, not in continuous space. Again the move is constrained to be a local one. The new trial permutation is obtained from the old permutation by applying a pair, triplet, or quadruplet permutation, for example $P' = p_{ij}P$, where p_{ij} is a pair permu-

tation of particles i and j. There is some evidence that pair permutations are energetically not favored and the Markov chain converges faster if triplet and quadruplet moves are permitted. A new permutation connecting points R_1 and R_2 a time t apart is sampled with a frequency proportional to

$$\langle R_1 \exp[-tH] p_{ij} P R_2 \rangle \,. \tag{3.4}$$

Co-ordinate moves follow up on that permutation move. Until the co-ordinate moves are made, it is not known whether that permutation move will be accepted. Details will be given elsewhere [7].

4. – Results.

Figure 1 shows the energy *vs.* temperature for liquid helium in the low-temperature region at saturated-vapor pressure. The solid curve gives the experimental results [8], the crosses the Monte Carlo ones with error bars of about 0.10 K, for a run of about 1 h on the CRAY-1. The Bose statistics have

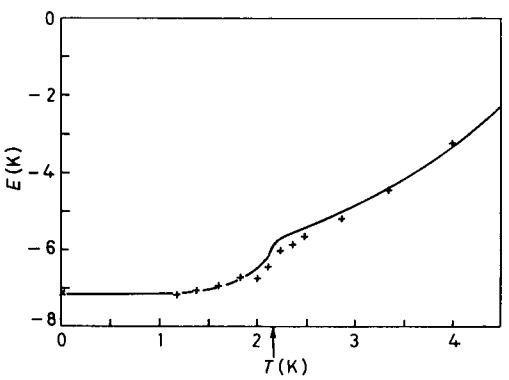

Fig. 1. – The internal energy in K/atom *vs.* the temperature at saturated-vapor pressure. The solid line is the experimental result [8]. The crosses are the results of the path integral Monte Carlo simulation with error bars of about 0.1 K. The × at zero temperature is the Green's function Monte Carlo result [3].

very little quantitative effect on the energy, less than 1 K. The point at zero temperature is the Green's function Monte Carlo result [3]. Except in the immediate vicinity of the transition, the path integral Monte Carlo results are accurate to 0.2 K, but lying systematically lower than the experimental results in the transition region. All of the simulations are performed with 64 atoms in periodic boundary conditions. There is numerical evidence that these boundary conditions favor permutations. The transition in the finite

system begins as soon as 2.5 K, whereas the experimental transition temperature is 2.17 K.

The comparison of the calculated specific heat with experiment at SVP is shown in fig. 2. The Monte Carlo results are obtained by taking finite differences of fig. 1. Thus the error bars are much larger. The results from using a fluctuation formula would have even larger error bars.

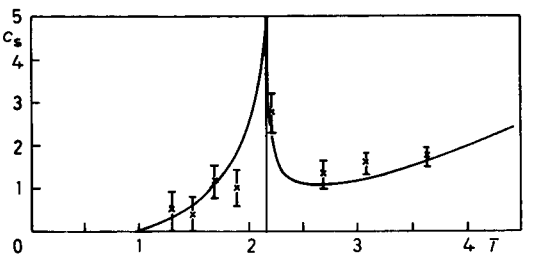

Fig. 2. – The specific heat per atom *vs.* the temperature. The curve is the experimental result [8]. The crosses with error bars are the finite differences of the Monte Carlo energies in fig. 1.

Figure 3 shows the pair correlation function at 2.08 K as obtained from X-ray scattering [9] at SVP, compared with the simulation results. They agree very well. Also shown is the effect of using Boltzmann statistics in the Monte Carlo calculation. This is obtained by not allowing permutation moves and increases the order in the liquid, raising the peak of the pair correlation

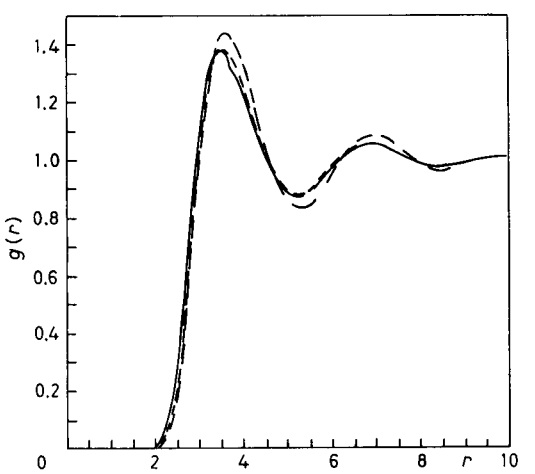

Fig. 3. – The pair correlation function for liquid helium at 2 K and SVP. The solid line is the X-ray scattering result [9]. The two dashed lines are the simulation results for bosons and for distinguishable atoms. The boson curve is the one lying very close to the experimental one.

function by 5%. There is similar agreement with scattering data at other densities and temperatures.

Although we have frequently referred to time slices, the simulation is actually in imaginary time, not real time. Nevertheless there is time-dependent information contained in the « dynamics » of these paths although it is smeared out because the motion is diffusive and not wavelike. Consider the dynamical structure factor $S(Q, w)$, measured by neutron scattering [10] and shown in fig. 4 at 1.2 K, for two wave vectors. There is a very large narrow peak cor-

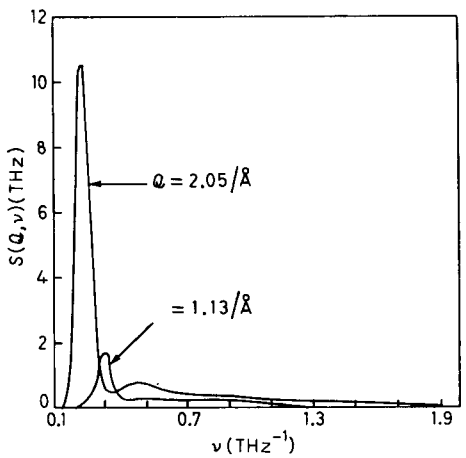

Fig. 4. – The dynamical structure factor at 1.2 K and SVP as measured by neutron scattering [10] for the two values of momentum transfer shown.

responding to single-phonon excitations, and a much broader multiphonon peak. Now in quantum Monte Carlo one can compute the imaginary-time density autocorrelation function

$$F(Q, t) = \mathrm{tr}\,[\varrho_Q \exp[-tH]\varrho_{-Q} \exp[-(\beta - t)H]]/\mathrm{tr}\,[\exp[-tH]]\,, \tag{4.1}$$

where

$$\varrho_Q = \sum_{i=1}^{N} \exp[-i\boldsymbol{Q}\boldsymbol{r}_i]/\sqrt{N}\,. \tag{4.2}$$

It can be shown by writing both $F(Q, t)$ and $S(Q, w)$ in their eigenfunction expansions that F is the Laplace transform of S:

$$F(Q, t) = \int_{-\infty}^{\infty} \mathrm{d}w \exp[-wt] S(Q, w)\,. \tag{4.3}$$

Inverse Laplace transforms are essentially impossible to perform with noisy

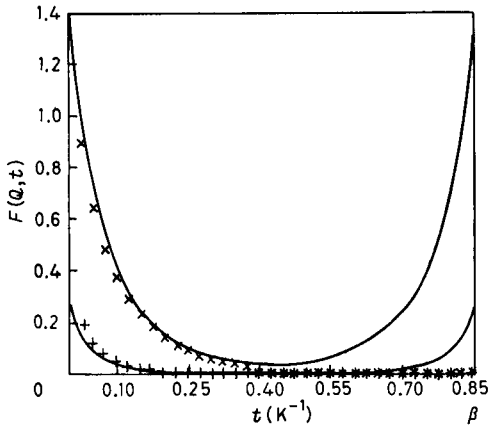

Fig. 5. – The Laplace transform of the experimental dynamical structure factor (× and +) in fig. 4 as compared with that calculated with path integral Monte Carlo (solid lines) for two values of momentum transfer.

data, thus we cannot go from F to S. The information has simply been lost with the Laplace transform. One could perform an inversion of F by assuming a functional form for $S(Q, w)$ with perhaps four unknown parameters, and using the values for $F(Q, t)$ to determine those parameters. It is very difficult to obtain more time-dependent information than this from the imaginary-time

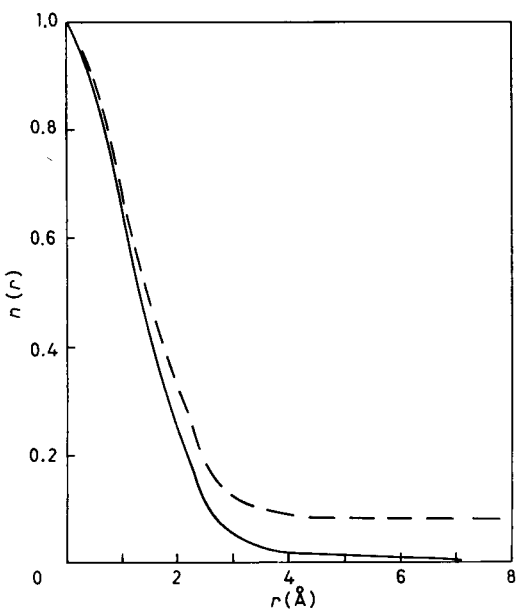

Fig. 6. – The single-particle density matrix at 2.86 K (solid line) and at 1.0 K (dashed line).

simulations. Since the experimental data are available, we can Laplace transform them and compare with the Monte Carlo results in imaginary time. This is done in fig. 5 with the data from fig. 4. The agreement is rather good both at this temperature and others where complete experimental data are available. The curves do differ at large values of t, because the experiments have not covered a wide enough range of energy transfers. The function F must be symmetric about $\beta/2$, and the Monte Carlo results are by definition.

The momentum distribution is of great interest since it is believed that many of the singular transport properties result from a finite fraction of the particles condensing into the zero-momentum state. Let $n(\boldsymbol{Q})$ be the probability of observing an atom with momentum $\boldsymbol{Q}$. It can be easily shown [11] that the Fourier transform of the momentum distribution is equal to the single-particle off-diagonal density matrix. Let

$$n(\boldsymbol{r}) = \int \mathrm{d}\boldsymbol{Q} \exp\left[i\boldsymbol{Q}\boldsymbol{r}\right] n(\boldsymbol{Q}) \,. \tag{4.4}$$

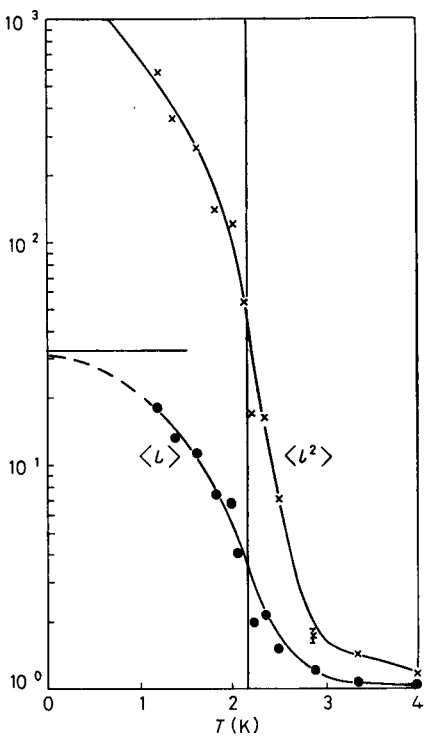

Fig. 7. – The average cycle length and squared cycle length of a permutation *vs.* the temperature at SVP. The vertical line at 2.17 K is the experimental transition temperature. For a random permutation of length N the average cycle length is $N/2$, marked for $N = 64$.

Then $n(\boldsymbol{r})$ is obtained as

$$n(\boldsymbol{r}) = \mathrm{tr}\,[\boldsymbol{r}_1, \boldsymbol{r}_2, \ldots, \exp[-\beta H]\boldsymbol{r}_1 + \boldsymbol{r}, \boldsymbol{r}_2, \ldots]/\mathrm{tr}\,[\exp[-\beta H]]\,, \tag{4.5}$$

where $\boldsymbol{r}_i$ is the co-ordinate of atom i. Atom 1 is off the diagonal, it does not return to its starting place but to a point r displaced. In the polymer analogy, $n(\boldsymbol{r})$ is obtained by cutting one of the polymers, and measuring the resulting end-to-end distribution. The polymers can still cross-link and this is responsible for momentum condensation. By adding other polymers into the middle of the one linear polymer, the ends can become arbitrarily far apart. Otherwise they would be restricted to a distance on the order of a thermal wavelength. End-to-end distributions computed in this way at 2.9 K and 1.0 K are shown in fig. 6. The curves fall off to a constant value apparently by 5 A. This constant value is the number of particles which have exactly zero momentum, since the Fourier transform of a constant function n_0 is $n_0\delta(Q)$. The calculations are in agreement with experiment [12] giving a condensate at low temperatures

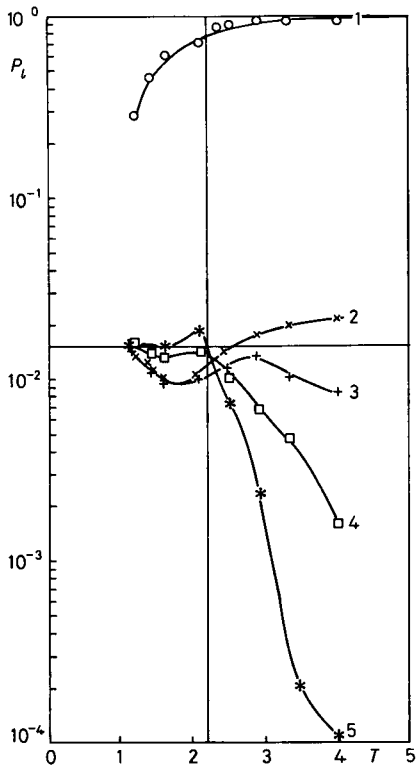

Fig. 8. – The distribution of cycles of length 1 to 5 as a function of temperature at SVP. The horizontal line shows the value expected for a random permutation of length 64.

of about 9%, but in this case the Monte Carlo results are more accurate than the experiment, since measuring the momentum distribution by neutron scattering is extremely difficult.

Statistics on the distribution of various permutation cycle lengths and of the mean and the mean squared cycle length are given in fig. 7, 8. They show a rapid rise in the number of longer permutations between 2.5 K and 2.0 K, and then a saturation to the value appropriate to a random permutation below that temperature. In a random permutation all cycle lengths are equally probable. At 2.25 K cycles of lengths 2, 3, 4 and 5 have approximately the same probability which is perhaps the clearest indication that the transition is occurring there.

* * *

E. L. POLLOCK has collaborated with the author on the work reported here. Work performed under the auspices of the U.S. Department of Energy by the Lawrence Livermore National Laboratory under contract number W-7405-ENG-48.

REFERENCES

[1] R. A. AZIZ, V. P. S. NAIN, J. S. CARLEY, W. L. TAYLOR and G. T. MCCONVILLE: *J. Chem. Phys.*, **70**, 4330 (1979).
[2] R. P. FEYNMAN: *Statistical Mechanics* (Benjamin, Reading, Mass., 1972).
[3] M. H. KALOS, M. A. LEE, P. A. WHITLOCK and G. V. CHESTER: *Phys. Rev. B*, **24**, 115 (1981).
[4] M. KAC: *Probability and Related Topics in Physical Science* (Interscience, New York, N. Y., 1959), p. 165.
[5] E. L. POLLOCK and D. M. CEPERLEY: *Phys. Rev. B*, **30**, 2555 (1984).
[6] N. METROPOLIS, A. W. ROSENBLUTH, M. N. ROSENBLUTH, A. H. TELLER and E. TELLER: *J. Chem. Phys.*, **21**, 1087 (1953).
[7] D. M. CEPERLEY and E. L. POLLOCK: *Phys. Rev. Lett.*, **56**, 351 (1986).
[8] R. K. CRAWFORD: in *Rare Gas Solids*, Vol. II, edited by M. L. KLEIN and J. A. VENABLES (Academic Press, New York, N. Y., 1977), p. 663.
[9] H. N. ROBKOFF and R. B. HALLOCK: *Phys. Rev. B*, **24**, 159 (1981).
[10] E. C. SVENSSON, P. MARTEL, V. F. SEARS and A. D. WOODS: *Can. J. Phys.*, **54**, 2178 (1976).
[11] O, PENROSE and L. ONSAGER: *Phys. Rev.*, **104**, 576 (1956).
[12] V. F. SEARS, E. C. SVENSSON, P. MARTEL and A. D. B. WOODS: *Phys. Rev. Lett.*, **49**, 279 (1982).

Reprinted From
Molecular-Dynamics Simulation of
Statistical-Mechanical Systems

Soc. Italiana di Fisica - Bologna - Italy